

Energy band gaps and lattice parameters evaluated with the Heyd-Sensieria-Ernzerhof screened hybrid functional

Jochen Heyd, Juan E. Peralta, and Gustavo E. Scuseria^{a)}
Department of Chemistry, Rice University, Houston, Texas 77005-1892

Richard L. Martin

Theoretical Division and Seaborg Institute for Transactinium Science, Los Alamos National Laboratory, Los Alamos, New Mexico 87545

(Received 4 August 2005; accepted 31 August 2005)

This work assesses the Heyd-Scuseria-Ernzerhof (HSE) screened Coulomb hybrid density functional for the prediction of lattice constants and band gaps using a set of 40 simple and binary semiconductors. An extensive analysis of both basis set and relativistic effects is given. Results are compared with established pure density functionals. For lattice constants, HSE outperforms local spin-density approximation (LSDA) with a mean absolute error (MAE) of 0.037 Å for HSE vs 0.047 Å for LSDA. For this specific test set, all pure functionals tested produce MAEs for band gaps of 1.0–1.3 eV, consistent with the very well-known fact that pure functionals severely underestimate this property. On the other hand, HSE yields a MAE smaller than 0.3 eV. Importantly, HSE correctly predicts semiconducting behavior in systems where pure functionals erroneously predict a metal, such as, for instance, Ge. The short-range nature of the exchange integrals involved in HSE calculations makes their computation notably faster than regular hybrid functionals. The current results, paired with earlier work, suggest that HSE is a fast and accurate alternative to established density functionals, especially for solid state calculations. © 2005 American Institute of Physics. [DOI: 10.1063/1.2085170]

I. INTRODUCTION

For many years, the local spin-density approximation¹ (LSDA) has reigned supreme for applications in solid-state physics. Structural properties such as lattice constants and bulk moduli are predicted with good accuracy. However, LSDA results for electronic properties such as band gaps are of much lower quality.² Improvements in density-functional theory (DFT) have first led to generalized-gradient approximations (such as the Perdew-Burke-Ernzerhof³ or PBE functional) and meta-generalized-gradient approximations (such as the Tao-Perdew-Staroverov-Scuseria⁴ or TPSS functional). The newer approaches do not necessarily improve all calculated properties.^{5,6} For example, predicted lattice constants are generally more accurate with LSDA than PBE or TPSS,⁶ and the severe underestimation of band gaps given by LSDA only improves marginally with these other functionals.

Several approaches that improve the band gaps predicted by LSDA have been developed. The most widely used in the solid-state physics community are the “scissor operator” approach,⁷ the LSDA+U,^{8–10} and Green’s-function-based methods, such as the GW approximation.¹¹ In contrast to LSDA, these approaches succeed in describing the band gaps of semiconductors, although in general they rely on LSDA-optimized lattice parameters.

There is a distinct need for a universally applicable method that does not contain any system-dependent param-

eters and is computationally feasible for a wide range of systems. Ideally, such a method would be equally suited for both molecules and solids, providing reliable results for predicted properties. Also, computing analytic energy derivatives is desirable. For molecules, hybrid functionals,¹² which include a portion of exact Hartree-Fock (HF) exchange, satisfy part of these requirements and consistently yield excellent results.^{13,14} However, there are two main issues concerning hybrid DFT calculations in solids. First, exact exchange interactions in three-dimensional metals are doomed to fail.¹⁵ Second, even for finite band-gap systems (where calculations are feasible), the CPU time requirement of traditional hybrid functionals is extremely high, especially for systems with small band gaps. The culprit for the limited applicability of traditional hybrid functionals in solid-state physics is the inherently long-range character of HF exchange.^{16–18} The decay of exact exchange interactions is highly band gap dependent. Systems with large gaps can be treated efficiently but convergence problems and demands for very large amounts of CPU time surface for semiconductors. These problems can be circumvented by employing a screened Coulomb potential for the exchange interaction. Such screened potentials have been previously proposed for solid-state physics calculations¹⁹ and also in quantum chemistry.^{20–24} A screened Coulomb potential is based on a splitting of the Coulomb operator into short-range (SR) and long-range (LR) components. The Heyd-Scuseria-Ernzerhof (HSE) hybrid functional^{14,17} employs a screened, short-range HF exchange

^{a)}Electronic mail: guscus@rice.edu

instead of the full exact exchange to avoid the problems mentioned above. In this way, metals, semiconductors, and insulators, as well as molecular systems, can be efficiently treated using the *same* approach.

The screened terms in HSE result from splitting the Coulomb operator into short- and long-range terms in the following fashion:

$$\frac{1}{r} = \underbrace{\frac{\text{erfc}(\omega r)}{r}}_{\text{SR}} + \underbrace{\frac{\text{erf}(\omega r)}{r}}_{\text{LR}}, \quad (1)$$

where the complementary error function $\text{erfc}(\omega r) = 1 - \text{erf}(\omega r)$ and ω determines the range. For $\omega=0$, the long-range term becomes zero and the SR term is equivalent to the full Coulomb operator. The opposite is the case for $\omega \rightarrow \infty$. The functional form of HSE is based on the PBEh hybrid functional (also known in the literature as PBE1PBE and PBE0).^{25,26} The expression for the HSE exchange-correlation energy is:

$$E_{xc}^{\text{HSE}} = aE_x^{\text{HF,SR}}(\omega) + (1-a)E_x^{\omega\text{PBE,SR}}(\omega) + E_x^{\omega\text{PBE,LR}}(\omega) + E_c^{\text{PBE}}, \quad (2)$$

where $E_x^{\text{HF,SR}}$ is the SR HF exchange. $E_x^{\omega\text{PBE,SR}}$ and $E_x^{\omega\text{PBE,LR}}$ are the short- and long-range components of the PBE exchange functional, ω is the splitting parameter, and $a=1/4$ is the HF mixing constant (determined analytically via perturbation theory^{27,28}). If $\omega=0$, HSE is equivalent to PBEh and if $\omega \rightarrow \infty$, HSE tends toward the pure PBE functional. A detailed derivation of the individual terms can be found in Refs. 14, 17, and 18. The HSE form can be viewed as an adiabatic connection functional only for the short-range portion of exchange, whereas long-range exchange and correlation are treated at the PBE generalized-gradient approximation (GGA) level.

The HSE functional has performed well in a number of previous studies. First, the effect of the screening parameter ω has been examined for a large number of enthalpies of formation.¹⁴ The ω dependence of this property was only slight, with a range of possible values ($0.15 a_0^{-1} < \omega < 0.30 a_0^{-1}$). This fact, coupled with preliminary results for solids, has previously led us to choose $\omega=0.15 a_0^{-1}$. This value is system independent. Both enthalpies of formation and various other predicted properties for molecules were observed to be on par with the best traditional hybrid functionals such as PBEh and Becke-3-Lee-Yang-Par²⁹ (B3LYP). In fact, preliminary evidence suggests³⁰ that the SR HF exchange accounts for nearly all the improved thermochemical results of hybrid functionals (compared to pure DFT functionals).

HSE was previously benchmarked on a set of 21 metallic, semiconducting, and insulating solids.¹⁸ Results for lattice constants, bulk moduli, and band gaps showed a substantial improvement over pure density functionals with only a modest increase in CPU time. HSE has also been successfully applied to a series of actinide oxide compounds,^{31,32} as well as semiconducting PtO (Ref. 33) and metallic PtN.³⁴

The universal applicability of HSE stands in stark contrast to both traditional hybrid functionals and other screened Coulomb approaches. An interesting, early attempt by Adamson *et al.*²⁰ and Gill *et al.*²¹ screened all Coulomb interactions in molecules but yielded results far from experiment. Other methods^{22,23,35} make use of the LR HF component and are thus not as suitable for solids. The work by Bylander and Kleinman³⁶ bears connection to the HSE functional but does not make use of the improvements found in GGA exchange-correlation functionals.

The goal of this study is an in-depth assessment of the HSE screened hybrid functional for the prediction of both lattice constants and band gaps in three-dimensional solids. To this end, we have selected a set of 40 simple and binary systems (mostly semiconductors) where experimental data is available. The following sections first outline the test set and computational methods. Then both basis set and relativistic effects are examined. Finally, we present results for the LSDA, PBE, TPSS, and HSE functionals and compare them.

II. THE SEMICONDUCTOR/40 TEST SET

Semiconducting materials are of great technological importance. The accurate prediction of both their structural and electronic properties has received much attention in the past decades. Nonetheless, the authors are not aware of a standard test set used to evaluate the performance of new methods for semiconductors (even though review articles such as Ref. 11 include some collected results). We therefore chose a set of semiconductors based on the following criteria: All considered systems were both closed shell and of simple or binary composition. We preferred solids with simple zinc-blende or rock salt structures but did include several systems with wurtzite structures. In addition, the availability of experimental data for lattice constants (and to a lesser extent band gaps) was an important factor.

These criteria led to the semiconductor/40(SC/40) set of 40 solids containing 13 group IIA-VI systems, 6 group IIB-VI systems, 17 group III-V systems, and 4 group IV systems. Table I contains a full list of all compounds and references to the experimental data shown in the Results section. A few systems with larger band gaps (diamond, BN, AlN, MgO, and MgS) were included since they otherwise fit into this systematic study. An effort was made to cross-check several experimental results and to cite the most recent data, but for some systems, only a single experimental source was available. Also, several experimental numbers are extrapolations from tertiary alloys. For our purposes, however, these results are still sufficiently accurate. The band gaps cited mostly correspond to the lowest excitation energy (direct or indirect gap). For systems with experimentally known spin-orbit splitting, the weighted average was used as the scalar-relativistic (i.e., neglecting spin-orbit coupling) band gap. The calculated band gaps, presented below, were obtained at the optimized structures for each functional. All experimental and optimized structures, as well as the basis sets used (see below), are available as supplementary material through the EPAPS depository.³⁷

TABLE I. Systems, structures, experimental references for the SC/40 set of semiconductors, and the Gaussian basis sets used in this work.

Solid	Structure	References	Basis set ^a
C	A2 diamond	48	1
Si	A2 diamond	48	1
Ge	A2 diamond	48	2
SiC	B3 zinc blende	48	1/1
BN	B3 zinc blende	49	1/1
BP	B3 zinc blende	48	1/1
BA _s	B3 zinc blende	50	1/2
BS _b	B3 zinc blende	48	1/2
AlN	B4 wurtzite	51	1/1
AlP	B3 zinc blende	52	1/1
AlAs	B3 zinc blende	52	1/2
AlSb	B3 zinc blende	53	1/2
GaN	B4 wurtzite	54	2/1
GaN	B3 zinc blende	55	2/1
GaP	B3 zinc blende	48	2/1
GaAs	B3 zinc blende	48	2/2
GaSb	B3 zinc blende	56	2/2
InN	B4 wurtzite	51 and 57	2/1
InP	B3 zinc blende	53	2/1
InAs	B3 zinc blende	53	2/2
InSb	B3 zinc blende	53	2/2
ZnS	B3 zinc blende	58 and 59	3/1
ZnSe	B3 zinc blende	58 and 59	3/2
ZnTe	B3 zinc blende	58 and 60	3/2
CdS	B3 zinc blende	58	3/1
CdSe	B3 zinc blende	58	3/2
CdTe	B3 zinc blende	58	3/2
MgO	B1 cubic	49	1/1
MgS	B3 zinc blende	61	1/1
MgSe	B1 cubic	62	1/2
MgTe	B3 zinc blende	63	1/2
CaS	B1 cubic	64	3/1
CaSe	B1 cubic	64	3/2
CaTe	B1 cubic	64	3/2
SrS	B1 cubic	65	3/1
SrSe	B1 cubic	65	3/2
SrTe	B1 cubic	66	3/2
BaS	B1 cubic	67 and 68	3/1
BaSe	B1 cubic	67 and 68	3/2
BaTe	B1 cubic	67 and 68	3/2

^a1=*m*-6-311G*, 2=*m*-pVDZ-PP, and 3=*m*-S-RSC (available in Ref. 37).

III. COMPUTATIONAL DETAILS

We have previously implemented the HSE functional into the GAUSSIAN suite of programs.³⁸ All calculations employed the periodic boundary-condition (PBC) code³⁹ available in GAUSSIAN. Three-dimensional, self-consistent, closed-shell spin-restricted Kohn-Sham calculations were performed on all systems. The short-range HF exchange interactions were calculated in real space using an adaptation of the NFX method⁴⁰ for periodic systems. Gaussian basis sets were used throughout this work.

All calculations converged the self-consistent field procedure to an accuracy of 10^{-8} hartree in the total energy per unit cell. SR exchange integrals smaller than 10^{-8} a.u. were neglected. This rather drastic cutoff is made possible by the guaranteed exponential decay of the short-range exchange

TABLE II. Basis set dependence for silicon. *m*-denotes a modified basis set (see text).

Basis	LSDA	PBE	TPSS	HSE
Lattice constant (Å)				
6-31G*	5.426	5.490	5.477	5.454
6-311G*	5.413	5.483	5.469	5.448
<i>m</i> -6-311G*	5.410	5.479	5.466	5.444
<i>m</i> -6-311G(2 <i>d</i>)	5.408	5.480	5.469	5.446
Band gap (eV)				
6-31G*	0.52	0.71	0.78	1.31
6-311G*	0.56	0.75	0.78	1.34
<i>m</i> -6-311G*	0.58	0.75	0.82	1.28
<i>m</i> -6-311G(2 <i>d</i>)	0.58	0.75	0.84	1.29

integrals. Even with this cutoff, total energies are accurate to 10^{-6} hartree. The numerical cutoffs typically used in periodic HF calculations with the full $1/r$ Coulomb potential (instead of the SR portion in HSE) have similar small effects, on total energies, at least in our code.⁴⁰ The reciprocal space integration was performed using at least 12 *k* points in each dimension for the pure density functionals and at least 24 *k* points in each dimension for the HSE hybrid functional.

All results were obtained on either dual processor AMD Athlon 1800+ or quad processor AMD Opteron 848 computers. CPU times for the geometry optimizations varied from a few hours to several days depending on the number of electrons and complexity of the system.

IV. RESULTS AND DISCUSSION

Our current work focuses on lattice parameters and band gaps of the systems in the SC/40 test set. Since we are using Gaussian-type basis sets and relativistic effects cannot be neglected in many systems of our test set, a closer look at both basis set and relativistic effects is in order.

A. Basis set and relativistic effects

All basis sets used are modified molecular Gaussian basis sets. Modifications are necessary since good-quality molecular basis sets normally include diffuse functions to model tails of wave functions that do not exist in solids. These diffuse functions unnecessarily slow down the calculations (making the Coulomb near field of the fast multipole method much slower),⁴¹ and may lead in some cases to numerical noise originating from the truncation scheme for exchange in solids. Diffuse exponents also heavily contribute to linear dependencies but these are eliminated in our program in the same way that it is done for molecules (i.e., diagonalizing the overlap matrix and removing combinations of basis functions whose eigenvalue is below a certain threshold). As a general rule, all basis functions in this work with exponents below 0.12 were removed. In cases where gaps between exponents were evidently too large, we added basis functions to produce an even-tempered series (for exponents less than 1.2). These modified basis sets are henceforth denoted with an *m*-prefix and available as supplementary material through the EPAPS depository.³⁷

TABLE III. Basis set dependence for germanium. *m*-denotes a modified basis set (set text).

Basis	Type	LSDA	PBE	TPSS	HSE
Lattice constant (Å)					
<i>m</i> -6-311G*	all electron	5.629	5.763	5.729	5.702
<i>m</i> -LANL2DZ	large-core RECP	5.824	5.848	5.856	5.788
<i>m</i> -LANL2DZdp	large-core RECP	5.794	5.814	5.819	5.765
<i>m</i> -Stuttgart-RLC	large-core RECP	5.822	5.853	5.871	5.785
<i>m</i> -cc-pVDZ-PP	small-core RECP	5.634	5.776	5.744	5.701
<i>m</i> -cc-pVTZ-PP	small-core RECP	5.640	5.778	5.738	5.705
<i>m</i> -cc-pVTZ	all electron, scalar relativistic	5.603	5.741	5.696	5.675
Band gap (eV)					
<i>m</i> -6-311G*	all electron	0.47	0.27	0.50	1.09
<i>m</i> -LANL2DZ	large-core RECP	0.44	0.33	0.38	1.23
<i>m</i> -LANL2DZdp	large-core RECP	0.56	0.62	0.76	1.28
<i>m</i> -Stuttgart-RLC	large-core RECP	0.00	0.00	0.00	0.19
<i>m</i> -cc-pVDZ-PP	small-core RECP	0.00	0.00	0.00	0.56
<i>m</i> -cc-pVTZ-PP	small-core RECP	0.00	0.00	0.00	0.59
<i>m</i> -cc-pVTZ	all electron, scalar relativistic	0.09	0.00	0.00	0.59

For the lighter elements in the SC/40 test set, a modified 6-311G* basis was chosen. Extensive tests on several systems showed this basis to be sufficient for structural parameters and band gaps. As an example, Table II shows the basis set dependence of the lattice constant and band gap for Silicon. Both properties are well converged with this basis. Notably, removing the diffuse functions (going from 6-311G* to *m*-6-311G*) only affected the results slightly.

Relativistic effects come into play for atoms in or below the fourth period. Thirty-one of the 40 systems studied here contain such elements. Therefore, the inclusion of relativistic effects has been examined. We compared nonrelativistic all-

electron calculations and both large- and small-core relativistic effective core potential (RECP) calculations. As a benchmark, scalar-relativistic all-electron calculations with a fully uncontracted *m*-cc-pVTZ basis set were used. Scalar-relativistic calculations were carried out using the Douglas-Kroll-Hess approximation⁴²⁻⁴⁴ as implemented for periodic systems in our group.⁴⁵ This all-electron full-potential approach allows the treatment of all electrons on an equal footing. All-electron scalar-relativistic calculations for solids are notably more demanding in terms of CPU requirements than its RECP counterparts. Moreover, as analytic forces are not yet available in our code for this case, numerical differentia-

TABLE IV. Comparison between the small-core RECP *m*-cc-pVDZ-PP and scalar-relativistic, all-electron calculations.

System	Type	LSDA	PBE	TPSS	HSE
Lattice constant (Å)					
Ge	RECP	5.634	5.776	5.744	5.701
	scalar relativistic, all electron	5.603	5.741	5.696	5.675
BAs	RECP	4.750	4.829	4.821	4.794
	scalar relativistic, all electron	4.731	4.809	4.800	4.772
GaAs	RECP	5.626	5.771	5.745	5.705
	scalar relativistic, all electron	5.601	5.744	5.710	5.683
InP	RECP	5.839	5.970	5.961	5.909
	scalar relativistic, all electron	5.814	5.943	5.936	5.887
Band gap (eV)					
Ge	RECP	0.00	0.00	0.00	0.56
	scalar relativistic, all electron	0.09	0.00	0.00	0.59
BAs	RECP	1.16	1.27	1.29	1.92
	scalar relativistic, all electron	1.19	1.29	1.29	1.88
GaAs	RECP	0.43	0.19	0.52	1.21
	scalar relativistic, all electron	0.53	0.19	0.49	1.22
InP	RECP	0.83	0.68	0.90	1.64
	scalar relativistic, all electron	0.78	0.66	0.87	1.57

TABLE V. Lattice constant (\AA) and band gap (eV) results for the SC/40 test set.

Solid	Lattice constants					Band gaps					
	LSDA	PBE	TPSS	HSE	Expt.	LSDA	PBE	TPSS	HSE	Expt.	
C	3.537	3.579	3.579	3.553	3.567	4.23	4.17	4.21	5.49	5.48	
Si	5.410	5.479	5.466	5.444	5.430	0.59	0.75	0.82	1.28	1.17	
Ge	5.634	5.776	5.744	5.701	5.658	0.00	0.00	0.00	0.56	0.74	
SiC	4.355	4.404	4.394	4.372	4.358	1.40	1.46	1.42	2.39	2.42	
BN	3.584	3.629	3.629	3.603	3.616	4.45	4.51	4.52	5.98	6.22	
BP	4.509	4.567	4.566	4.543	4.538	1.31	1.41	1.45	2.16	2.4	
BAs	4.750	4.829	4.821	4.794	4.777	1.16	1.27	1.29	1.92	1.46	
BSb	5.201	5.291	5.280	5.251	n/a	0.80	0.88	0.81	1.37	n/a	
AlN	(a)	3.112	3.153	3.147	3.127	3.111	4.98	4.95	5.01	6.45	6.13
	(c)	4.974	5.045	5.028	5.000	4.981					
AlP	5.436	5.508	5.497	5.472	5.463	1.60	1.83	1.90	2.52	2.51	
AlAs	5.639	5.733	5.713	5.691	5.661	1.40	1.62	1.71	2.24	2.23	
AlSb	6.079	6.188	6.172	6.146	6.136	1.29	1.40	1.63	1.99	1.68	
GaN	(a)	3.167	3.233	3.224	3.198	3.189	2.09	1.70	1.73	3.21	3.50
	(c)	5.165	5.272	5.244	5.204	5.185					
β -GaN	4.476	4.569	4.552	4.518	4.523	1.93	1.55	1.56	3.03	3.30	
GaP	5.418	5.534	5.522	5.484	5.451	1.59	1.71	1.98	2.47	2.35	
GaAs	5.626	5.771	5.745	5.705	5.648	0.43	0.19	0.52	1.21	1.52	
GaSb	6.043	6.208	6.183	6.140	6.096	0.09	0.00	0.08	0.72	0.73	
InN	(a)	3.523	3.599	3.589	3.555	3.537	0.02	0.01	0.00	0.71	0.69
	(c)	5.684	5.807	5.765	5.729	5.704					
InP	5.839	5.970	5.961	5.909	5.869	0.83	0.68	0.90	1.64	1.42	
InAs	6.038	6.195	6.170	6.120	6.058	0.00	0.00	0.00	0.39	0.41	
InSb	6.430	6.608	6.585	6.535	6.479	0.00	0.00	0.00	0.29	0.23	
ZnS	5.319	5.467	5.465	5.432	5.409	2.25	2.16	2.39	3.42	3.66	
ZnSe	5.588	5.751	5.736	5.707	5.668	1.21	1.19	1.48	2.32	2.70	
ZnTe	6.017	6.195	6.174	6.150	6.089	1.28	1.14	1.45	2.19	2.38	
CdS	5.776	5.934	5.944	5.896	5.818	1.01	1.11	1.34	2.14	2.55	
CdSe	6.025	6.210	6.195	6.152	6.052	0.34	0.48	0.73	1.39	1.90	
CdTe	6.422	6.626	6.610	6.568	6.480	0.61	0.62	0.88	1.52	1.92	
MgO	4.178	4.268	4.247	4.218	4.207	4.92	4.34	4.56	6.50	7.22	
MgS	5.618	5.721	5.719	5.681	5.622	3.54	3.57	3.88	4.78	5.4	
MgSe	5.417	5.532	5.520	5.499	5.40	1.70	1.76	2.07	2.62	2.47	
MgTe	6.381	6.517	6.517	6.478	6.42	2.74	2.68	3.12	3.74	3.6	
CaS	5.572	5.715	5.710	5.698	5.689	2.16	2.56	2.69	3.59	n/a	
CaSe	5.799	5.962	5.955	5.946	5.916	1.74	2.11	2.23	3.02	n/a	
CaTe	6.209	6.387	6.386	6.381	6.348	1.25	1.60	1.72	2.37	n/a	
SrS	5.926	6.066	6.052	6.037	5.99	2.27	2.68	2.79	3.59	n/a	
SrSe	6.151	6.306	6.290	6.282	6.234	1.89	2.26	2.37	3.09	n/a	
SrTe	6.543	6.714	6.703	6.701	6.64	1.51	1.89	2.00	2.57	n/a	
BaS	6.303	6.436	6.433	6.413	6.389	2.05	2.44	2.61	3.28	3.88	
BaSe	6.517	6.671	6.659	6.649	6.595	1.76	2.12	2.26	2.87	3.58	
BaTe	6.897	7.062	7.062	7.051	7.007	1.49	1.87	2.01	2.50	3.08	

tion has been carried out to obtain the minimum-energy lattice constant (see Ref. 45 for further details), making the computations even more demanding. Therefore, we limit this benchmark to four representative systems: Ge, BAs, GaAs, and InP (for In, a modified universal Gaussian basis set was employed).⁴⁶

In the case of Ge (Table III), a nonrelativistic m -6-311G* calculation leads to acceptable lattice constants. However, the predicted band gap is significantly overestimated. Large-core RECPs (Ar core) are not suitable since lattice constants are overestimated by up to 0.2 \AA . Small-core RECPs (Ne core), on the other hand, perform quite well for both lattice constants and band gaps. Tests using a triple-zeta

valence basis set did not change the results in any significant way. Further evidence from BAs, GaAs, and InP is shown in Table IV. The agreement with all-electron scalar-relativistic calculations is good throughout. However, these tests indicate that even calculations using available small-core RECPs tend to overestimate the lattice constants by about 0.02 \AA . On the other hand, the small-core RECP approach delivers essentially the same band gaps as the all-electron scalar-relativistic approach.

In summary, we chose a modified m -6-311G* basis for the lighter elements and small-core RECPs with a double-zeta valence basis set [m -cc-pVDZ-PP (Ref. 47) or m -Stuttgart-RSC-1997] for the heavier elements. Most of

TABLE VI. Lattice constant error statistics for the SC/40 test set (Å).

Solid	LSDA	PBE	TPSS	HSE
ME ^a	-0.046	0.076	0.063	0.035
MAE ^b	0.047	0.076	0.063	0.037
rms ^c	0.058	0.084	0.071	0.044
Max (+) ^d	0.017	0.158	0.143	0.100
Max (-) ^e	0.139	-0.014

^aMean error.^bMean absolute error.^cRoot-mean-square error.^dMaximum positive deviation.^eMaximum negative deviation.

these molecular basis sets needed to be modified to make them suitable for calculations in solids (See Ref. 37).

B. Lattice constants

Table V shows detailed results for all systems in the SC/40 test. Table VI contains the error statistics for predicting lattice constants with the four functionals studied in this work. In general, LSDA underestimates lattice constants in nearly all cases while PBE and TPSS always overestimate them. The screened hybrid functional HSE reduces the overestimation of PBE (on which it is based) drastically, leading to the best predictions overall. The mean absolute errors (MAEs) for the four functionals are 0.047, 0.076, 0.063, and 0.037 Å for LSDA, PBE, TPSS, and HSE, respectively. All other error measures paint a similar picture.

The 20% accuracy improvement of HSE over LSDA is noteworthy since LSDA is the most widely used method for lattice optimizations in solids. In addition, the overestimation of lattice constants by using RECPs (mentioned in the previous section) is partly responsible for the observed errors with HSE. We therefore expect scalar-relativistic all-electron calculations to yield even better results with HSE while the underestimation exhibited by LSDA would only be exaggerated in this case.

C. Band gaps

It is well known that all three nonhybrid density functionals examined here severely underestimate band gaps.² The MAEs for LSDA, PBE, and TPSS are 1.14, 1.25, and 1.12 eV, respectively. Band gaps calculated with these functionals are always underestimated, in extreme cases such as

TABLE VII. Band gap error statistics for the SC/40 test set (eV).

Solid	LSDA	PBE	TPSS	HSE
ME ^a	-1.14	-1.13	-0.98	-0.17
MAE ^b	1.14	1.13	0.98	0.26
rms ^c	1.24	1.25	1.12	0.34
Max (+) ^d	0.32
Max (-) ^e	-2.30	-2.88	-2.66	-0.72

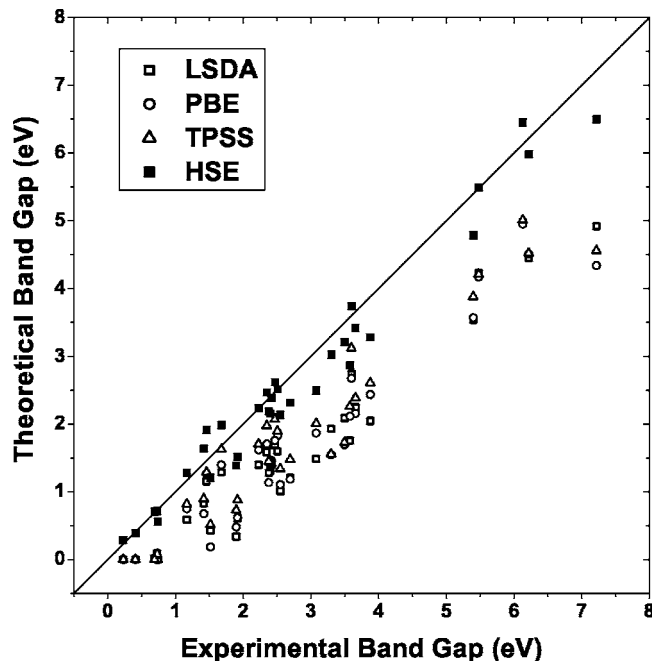
^aMean error.^bMean absolute error.^cRoot-mean-square error.^dMaximum positive deviation.^eMaximum negative deviation.

FIG. 1. A comparison of experimental band gaps for the SC/40 set with values computed with four different generations of DFT. The local spin-density approximation (LSDA), a generalized-gradient approximation (PBE), a meta-GGA (TPSS), and the hybrid functional HSE.

MgO, by as much as 2.88 eV. In addition, several small-band-gap systems (Ge, GaSb, InN, InAs, and InSb) are predicted to be quasimetallic. Detailed results can be found in Table V while the error statistics are summarized in Table VII. All band gaps correspond to lattices optimized with the respective functional. Band gaps at experimental lattices (available as supplementary material through the EPAPS depository, Ref. 37 show no significant differences from the results reported here.

On the other hand, the HSE hybrid functional yields a drastically reduced MAE of only 0.26 eV and predicts even small-band-gap systems correctly. A plot of all theoretical versus experimental band gaps is shown in Fig. 1, illustrating the performance difference between HSE and the pure density functionals. The HSE errors for band gaps are comparable to those obtained with the GW approximation.¹¹ However, two important points need to be raised to put these results into perspective. First, none of our calculations include any excitonic or quasiparticle effects. While these effects are small for some systems, they can be non-negligible for others. Second, some systems in the SC/40 test set exhibit significant spin-orbit coupling effects which can split the band gap by up to 1 eV (for example, ZnTe). For these systems, we are comparing the weighted average of the split experimental bandgap, but a better description of the systems is highly desirable. Currently, efforts are underway to address the above concerns.

V. CONCLUSIONS

This work assesses the screened Coulomb hybrid functional HSE on a set of 40 solids with optical band gaps ranging from 0.2 to 7.2 eV and compares its performance to several pure density functionals. HSE offers both improved

lattice constants compared to LSDA and significantly improved band gaps. Especially for lattice constants, small-core RECPs are necessary to reproduce the scalar relativistic all-electron benchmarks.

The computational effort involved in HSE calculations presents only a modest increase (a factor of less than 2) over pure DFT calculations. All individual geometry optimizations in this study were completed in a matter of days on commodity hardware. Given the vast improvement in accuracy, such an extra effort is certainly justified.

It is encouraging that the HSE functional leads to much improved “frozen orbital” approximations to the band gap. However, we should point out that there is no *a priori* reason to expect a band calculation to precisely reproduce experimental band gaps.

In summary, the HSE functional is universally applicable and does not contain any system-dependent parameter. It yields excellent results, in molecules and solids, for many different properties. In contrast to other methods, HSE can be employed for both structural and electronic structure properties. Therefore, HSE provides a unique and powerful alternative for the study of large complex systems, such as chemisorption at surfaces and three-dimensional impurities in semiconductors.

ACKNOWLEDGMENTS

This work was supported by the Department of Energy (Grant No. DE-FG02-01ER15232) and the National Science Foundation (CHE-0457030). In addition, one of the authors (RLM) is grateful for support from the DOE OBES Heavy Element Program and the LDRD Program at Los Alamos National Laboratory.

- ¹W. Kohn and L. J. Sham, *Phys. Rev.* **140**, A1133 (1965).
- ²J. Perdew, *Int. J. Quantum Chem.* **30**, 451 (1986).
- ³J. P. Perdew, K. Burke, and M. Ernzerhof, *Phys. Rev. Lett.* **77**, 3865 (1996).
- ⁴J. Tao, J. P. Perdew, V. N. Staroverov, and G. E. Scuseria, *Phys. Rev. Lett.* **91**, 146401 (2003).
- ⁵V. N. Staroverov, G. E. Scuseria, J. Tao, and J. P. Perdew, *J. Chem. Phys.* **119**, 12129 (2003).
- ⁶V. N. Staroverov, G. E. Scuseria, J. Tao, and J. P. Perdew, *Phys. Rev. B* **69**, 075102 (2004).
- ⁷G. Baraff and M. Schlüter, *Phys. Rev. B* **30**, 3460 (1984).
- ⁸V. I. Anisimov, J. Zaanen, and O. K. Andersen, *Phys. Rev. B* **44**, 943 (1991).
- ⁹V. I. Anisimov, I. V. Solovyev, M. A. Korotin, M. T. Czyzyk, and G. A. Sawatzky, *Phys. Rev. B* **48**, 16929 (1993).
- ¹⁰A. I. Lichtenstein, J. Zaanen, and V. I. Anisimov, *Phys. Rev. B* **52**, R5467 (1995).
- ¹¹W. G. Aulbur, L. Jonsson, and J. W. Wilkins, *Solid State Phys.* **54**, 1 (2000).
- ¹²A. D. Becke, *J. Chem. Phys.* **98**, 1372 (1993).
- ¹³L. A. Curtiss, K. Raghavachari, P. C. Redfern, and J. A. Pople, *J. Chem. Phys.* **106**, 1063 (1997).
- ¹⁴J. Heyd and G. E. Scuseria, *J. Chem. Phys.* **120**, 7274 (2004).
- ¹⁵N. W. Ashcroft and N. D. Mermin, *Solid State Physics* (Saunders College, Orlando, Florida, 1976), p. 335.
- ¹⁶W. Kohn, *Int. J. Quantum Chem.* **56**, 229 (1995).
- ¹⁷J. Heyd, G. E. Scuseria, and M. Ernzerhof, *J. Chem. Phys.* **118**, 8207 (2003).
- ¹⁸J. Heyd and G. E. Scuseria, *J. Chem. Phys.* **121**, 1187 (2004).
- ¹⁹D. Pines, *Elementary Excitations in Solids* (Perseus Books, Reading, Massachusetts, 1999).
- ²⁰R. D. Adamson, J. P. Dombroski, and P. M. W. Gill, *Chem. Phys. Lett.* **254**, 329 (1996).
- ²¹P. M. W. Gill, R. D. Adamson, and J. A. Pople, *Mol. Phys.* **88**, 1005 (1996).
- ²²A. Savin, *Recent Developments and Applications of Modern Density Functional Theory* (Elsevier Science, New York, 1996), pp. 327–357.
- ²³H. Iikura, T. Tsuneda, T. Yanai, and K. Hirao, *J. Chem. Phys.* **115**, 3540 (2001).
- ²⁴A. Seidl, A. Görling, P. Vogl, and J. A. Majewski, *Phys. Rev. B* **53**, 3764 (1996).
- ²⁵M. Ernzerhof and G. E. Scuseria, *J. Chem. Phys.* **110**, 5029 (1999).
- ²⁶C. Adamo and V. Barone, *J. Chem. Phys.* **110**, 6158 (1999).
- ²⁷D. C. Langreth and J. P. Perdew, *Solid State Commun.* **17**, 1425 (1975).
- ²⁸J. P. Perdew, M. Ernzerhof, and K. Burke, *J. Chem. Phys.* **105**, 9982 (1996).
- ²⁹A. D. Becke, *J. Chem. Phys.* **98**, 5648 (1993).
- ³⁰O. Vydrov, J. Heyd, and G. E. Scuseria (unpublished).
- ³¹I. D. Prodan, G. E. Scuseria, J. A. Sordo, K. N. Kudin, and R. L. Martin, *J. Chem. Phys.* (in press).
- ³²I. D. Prodan, G. E. Scuseria, and R. L. Martin (unpublished).
- ³³J. Uddin, J. E. Peralta, and G. E. Scuseria, *Phys. Rev. B* **71**, 155112 (2005).
- ³⁴J. Uddin and G. E. Scuseria, *Phys. Rev. B* **72**, 035101 (2005).
- ³⁵T. Yanai, D. P. Tew, and N. C. Handy, *Chem. Phys. Lett.* **393**, 51 (2004).
- ³⁶D. M. Bylander and L. Kleinman, *Phys. Rev. B* **41**, 7868 (1990).
- ³⁷See EPAPS Document No. E-JCPA6-123-301539 for our detailed results for experimental and optimized structures, as well as calculated bandgaps and basis sets used. This document can be reached via a direct link in the online article’s HTML reference section or via the EPAPS homepage (<http://www.aip.org/pubservs/epaps.html>).
- ³⁸M. J. Frisch, G. W. Trucks, H. B. Schlegel, *et al.*, *Gaussian Development Version, Revision C.01* (Gaussian, Inc., Pittsburgh PA, 2004).
- ³⁹K. N. Kudin and G. E. Scuseria, *Phys. Rev. B* **61**, 16440 (2000).
- ⁴⁰J. C. Burant, G. E. Scuseria, and M. J. Frisch, *J. Chem. Phys.* **105**, 8969 (1996).
- ⁴¹M. C. Strain, G. E. Scuseria, and M. J. Frisch, *Science* **271**, 51 (1996).
- ⁴²M. Douglas and N. M. Kroll, *Ann. Phys.* **82**, 89 (1974).
- ⁴³B. A. Hess, *Phys. Rev. A* **32**, 756 (1985).
- ⁴⁴B. A. Hess, *Phys. Rev. A* **33**, 3742 (1986).
- ⁴⁵J. E. Peralta, J. Uddin, and G. E. Scuseria, *J. Chem. Phys.* **122**, 084108 (2005).
- ⁴⁶G. L. Malli, A. B. F. Da Silva, and Y. Ishikawa, *Phys. Rev. A* **47**, 143 (1993).
- ⁴⁷B. Metz, H. Stoll, and M. Dolg, *J. Chem. Phys.* **113**, 2563 (2000).
- ⁴⁸O. Madelung, *Semiconductors-Basic Data* 2nd ed. (Springer, New York, 1996).
- ⁴⁹B. Rafferty and L. M. Brown, *Phys. Rev. B* **58**, 10326 (1998).
- ⁵⁰R. M. Wentzcovitch and M. L. Cohen, *J. Phys. C* **19**, 6791 (1986).
- ⁵¹Q. Guo and A. Yoshida, *Jpn. J. Appl. Phys., Part 1* **33**, 2453 (1994).
- ⁵²B. Monemar, *Phys. Rev. B* **8**, 5711 (1973).
- ⁵³X. Zhu and S. G. Louie, *Phys. Rev. B* **43**, 14142 (1991).
- ⁵⁴B. Monemar, *Phys. Rev. B* **10**, 676 (1974).
- ⁵⁵G. Ramírez-Flores, H. Navarro-Contreras, and A. Lastras-Martínez, *Phys. Rev. B* **50**, 8433 (1994).
- ⁵⁶M. Levinstein, S. Romyantsev, and M. Shur, *Semiconductor Parameters* (World Scientific, Singapore, 1996).
- ⁵⁷B. Arnaudov, T. Paskova, P. P. Paskov, B. Magnusson, E. Valcheva, B. Monemar, H. Lu, W. J. Schaff, H. Amano, and I. Akasaki, *Phys. Rev. B* **69**, 115216 (2004).
- ⁵⁸O. Zakharov, X. Rubio, X. Blase, M. L. Cohen, and S. G. Louie, *Phys. Rev. B* **50**, 10780 (1994).
- ⁵⁹U. Lunz, C. Schumacher, J. Nürnberger, K. Schüll, A. Gerhard, U. Schüssler, B. Jobst, W. Faschinger, and G. Landwehr, *Semicond. Sci. Technol.* **12**, 970 (1997).
- ⁶⁰W. Walukiewicz, W. Shan, K. M. Yu, J. W. Ager III, E. E. Haller, I. Miotkowski, M. J. Seong, H. Alawadhi, and A. K. Ramdas, *Phys. Rev. Lett.* **85**, 1552 (2000).
- ⁶¹D. Wolverson, D. M. Bird, C. Bradford, K. A. Prior, and B. C. Cavenett, *Phys. Rev. B* **64**, 113203 (2001).
- ⁶²D. Rached, N. Benkhetou, B. Soudini, B. Abbar, N. Sekkal, and M. Driz, *Phys. Status Solidi B* **240**, 565 (2003).
- ⁶³J. M. Hartmann, J. Cibert, F. Kany, H. Mariette, M. Charleux, P. Alleysson, R. Langer, and G. Feuillet, *J. Appl. Phys.* **80**, 6257 (1996).
- ⁶⁴H. Luo, R. G. Greene, K. Ghandehari, T. Li, and A. L. Ruoff, *Phys. Rev. B* **50**, 16232 (1994).

⁶⁵H. Luo, R. G. Greene, and A. L. Ruoff, Phys. Rev. B **49**, 15341 (1994).

⁶⁶H. G. Zimmer, H. Winzen, and K. Syassen, Phys. Rev. B **32**, 4066 (1985).

⁶⁷G. Kalpana, B. Palanivel, and M. Rajagopalan, Phys. Rev. B **50**, 12318 (1994).

⁶⁸R. J. Zollweg, Phys. Rev. **111**, 113 (1958).

PROOF COPY 301539JCP